

THEORETICAL STRESS CONDITIONS IN THE MATRIX AROUND A RIGID CIRCULAR INCLUSION AND THEIR GEOLOGICAL IMPLICATIONS¹

KHANDEKER MOSHARRAF HOSSAIN²

ABSTRACT

Hossain, K. M. (1978). Theoretical stress conditions in the matrix around a rigid circular inclusion and their geological implications. *Geol. Mijnbouw*, 57, p. 55-58.

Equations are derived which describe the stress condition in the matrix around a rigid circular inclusion subjected to uniaxial stress. The values of the principal stresses and their orientations are obtained using a computer. The orientation of potential fractures around an inclusion is determined from the stress trajectories and the development of pressure shadows and pressure fringes are predicted by assuming that mineral migration occurs in response to gradients in the mean stress. The type of structures (whether pressure shadows or pressure fringes) that develop in the low mean stress zone adjacent to the inclusions is controlled by the magnitude of applied stress.

INTRODUCTION

Any rigid or semi-rigid object (e.g. porphyroblast, pebble, worm-tube, fossil etc.) embedded in a rock matrix undergoing deformation sets up stress variations around itself. This stress variation produces local deformation which often results in the formation of structures such as 'pressure shadows', 'pressure fringes', 'halo de etirement' and 'streckungshofe' (KNOPF, 1929; PABST, 1931; BAIN, 1933; MILES, 1945; FAIRBAIRN, 1950; FRANKEL, 1957; RAMSAY, 1967; JOPLIN, 1968; SPRY, 1969; and STRÖMGÅRD, 1972). Depending on its position in the matrix, an initially planar structure may become deformed around an inclusion or be protected from deformation by the inclusion. These protected, relatively low strain regions around a rigid inclusion are the areas where pressure shadows or pressure fringes develop.

Pressure fringe is a term used to describe the texture arising

from the growth of new minerals adjacent to a rigid object as a result of the pulling away of the material from the contact of the object. The shadows are characterized by the influx of new minerals into certain regions of the matrix around an inclusion. These minerals have no preferred orientation. As well as pressure shadows and pressure fringes, fracture patterns may also develop in the matrix around an inclusion undergoing deformation. This paper presents a theoretical study of the stress conditions in the matrix around a rigid inclusion. The analysis of the results is undertaken with a view to interpreting the development of the structures associated with the stress conditions.

It follows from Saint Venants' principle that any disturbance in the matrix around a rigid inclusion will be confined to the neighbourhood of the inclusion. It is assumed that the matrix material is homogeneous and has the ideal properties of linear elasticity. It is also assumed that the matrix material is firmly attached to the boundary of the included object so that the continuity of stress and displacement is maintained.

General solution

Consider that a circular inclusion inside a homogeneous ma-

¹ Manuscript received: 1977-08-31.

Revised manuscript received and accepted: 1977-11-09.

² Department of Geology, Dacca University, DACCA-2, Bangladesh.

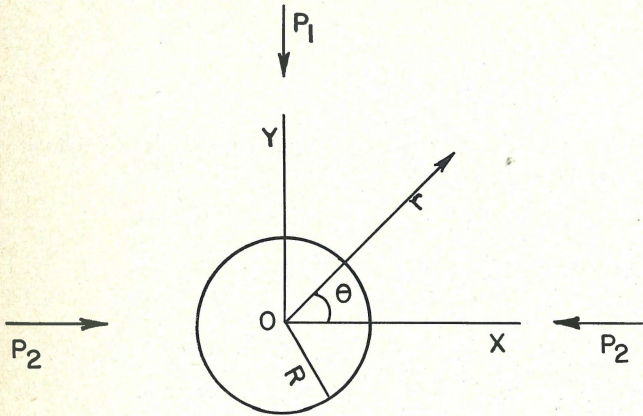


Fig. 1
A rigid circular inclusion under uniform stress from infinity: definition of variables used for the calculation.

trix be subjected to a uniform stress P_1 along the OY direction and P_2 along the OX direction (Fig. 1). For the case of uniaxial stress, P_2 is zero. 'r' and ' θ ' are the parameters of polar co-ordinates and 'R' is the radius of the circular inclusion. The shear modulus and Poisson's ratio of the matrix are 'G' and ' ν ' respectively and those of the inclusion are ' G_i ' and ' ν_i ' respectively.

The stresses in an infinite matrix containing no inclusion can be represented by the standard stress function [$\Phi(Z)$ and $\Psi(Z)$] (JAEGER & COOK, 1969, p. 236):

$$\begin{aligned} \Phi(Z) &= \frac{1}{4} P_1 Z \\ \Psi(Z) &= -\frac{1}{2} P_1 Z \end{aligned} \quad \dots \dots \dots (1)$$

If the matrix material contains a circular inclusion, some terms must be added to the above function to represent the effect of the inclusion (JAEGER & COOK, 1969). The equation (1) becomes:

$$\begin{aligned} \Phi(Z) &= \frac{1}{4} P_1 \left(Z + \frac{A}{Z} R^2 \right) \\ \Psi(Z) &= -\frac{1}{2} P_1 \left(Z + \frac{B}{Z} R^2 + \frac{C}{Z^3} R^3 \right) \end{aligned} \quad \dots \dots \dots (2)$$

where A, B and C are the real constants. Similarly, the stress function in the region inside the inclusion [$\Phi_i(Z)$ and $\Psi_i(Z)$] can be expressed as:

$$\begin{aligned} \Phi_i(Z) &= \frac{1}{4} P_1 \left(A_i Z + \frac{B_i}{R^2} Z^3 \right) \\ \Psi_i(Z) &= -\frac{1}{2} P_1 C_i Z \end{aligned} \quad \dots \dots \dots (3)$$

where A_i , B_i and C_i are the real constants inside the inclusion.

Using equations (2) and (3) and the standard equation for displacements, the relationship at the boundary (u_r and ν_r) and inside the inclusion (u_{ri} and ν_{ri}) can be obtained i.e.:

$$4G(u_r + \nu_r)/P_1 R = \frac{1}{2}(\eta - 1) + B + \left(\frac{1}{2}\eta A + 1\right)e^{-2i\theta} + \left(\frac{1}{2}A + C\right)e^{2i\theta} \quad \dots \dots \dots (4)$$

and

$$4G_i(u_{ri} + \nu_{ri})/P_1 R = \frac{1}{2}A_i(\eta_i - 1) + \frac{1}{2}\eta_i B_i e^{2i\theta} + (C_i - \frac{3}{2}B) e^{-2i\theta} \quad \dots \dots \dots (5)$$

where $\eta = 3 - 4\nu$ and $\eta_i = 3 - 4\nu_i$.

Equating the co-efficient of equations (4) and (5) and writing $K = G_i/G$, gives:

$$\begin{aligned} K(\eta - 1 + 2B) &= A_i(\eta_i - 1) \\ K(\eta A + 2) &= 2C_i - 3B_i \\ K(A + 2C) &= \eta_i B_i \end{aligned} \quad \dots \dots \dots (6)$$

Differentiating eqs. (2) and (3) and substituting in the standard function the required equations for the difference of normal and tangential stress at the boundary (N-iT) and inside the inclusion (N-iT) are obtained respectively as:

$$2(N-iT)/P_1 = 1 - B - \left(\frac{3}{2}A + 3C\right)e^{-2i\theta} + \left(1 - \frac{1}{2}A\right)e^{2i\theta} \quad \dots \dots \dots (7)$$

and

$$2(N-iT)/P_1 = A_i + \left(C_i - \frac{3}{2}B_i\right)e^{2i\theta} + \frac{3}{2}B_i e^{2i\theta} \quad \dots \dots \dots (8)$$

Now equating the co-efficient of equations (7) and (8) we obtain:

$$\begin{aligned} A_i &= 1 - B \\ B_i &= -A - 2C \\ 2C_i - 3B_i &= 2 - A. \end{aligned} \quad \dots \dots \dots (9)$$

From equations (6) and (9), the final solution for the real constants can be determined:

$$\begin{aligned} A_i &= K(\eta + 1)/(2K + \eta_i - 1) \\ B_i &= 0 \\ C_i &= K(\eta + 1)/(K\eta + 1) \end{aligned} \quad \dots \dots \dots (10)$$

and

$$\begin{aligned} A &= 2(1 - K)/(K\eta + 1) \\ B &= [\eta_i - 1 - K(\eta - 1)]/(2K + \eta_i - 1) \\ C &= (K - 1)/(K\eta + 1). \end{aligned} \quad \dots \dots \dots (11)$$

The general solution for the stress distribution can be obtained from the relationship between the resolved stresses (σ_r , σ_θ & $\tau_{r\theta}$) and the stress function:

$$\begin{aligned} \sigma_r &= \frac{1}{2}P_1 \left(1 - \frac{br\frac{1}{4}}{r^2} \right) + \frac{1}{2}P_1 \left(1 - \frac{2AR^2}{r^2} - \frac{3CR^4}{r^4} \right) \cos 2\theta \\ \sigma_\theta &= \frac{1}{2}P_1 \left(1 + \frac{BR^2}{r^2} \right) - \frac{1}{2}P_1 \left(1 - \frac{3CR^4}{r^4} \right) \cos 2\theta \\ \tau_{r\theta} &= -\frac{1}{2}P_1 \left(1 + \frac{AR^2}{r^2} + \frac{3CR^4}{r^4} \right) \sin 2\theta \end{aligned} \quad \dots \dots \dots (12)$$

Solution for the rigid circular inclusion

The rigidity contrast 'K' in this case is infinity, as the matrix material is assumed to be ductile. For non-compressible material $\nu = \frac{1}{2}$ and hence $\eta = 1$ (as $\eta = 3 - 4\nu$). Similarly $\eta_i = 1$.

Now substituting $K = \alpha$, $\eta = 1$ and $\eta_i = 1$ into eq. (11), the

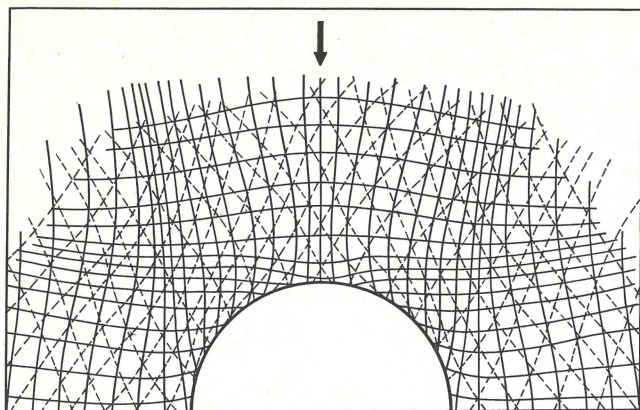


Fig. 2
Principal stress trajectories (solid lines) and predicted fracture pattern (Broken lines) around a rigid circular inclusion under applied uniaxial stress.

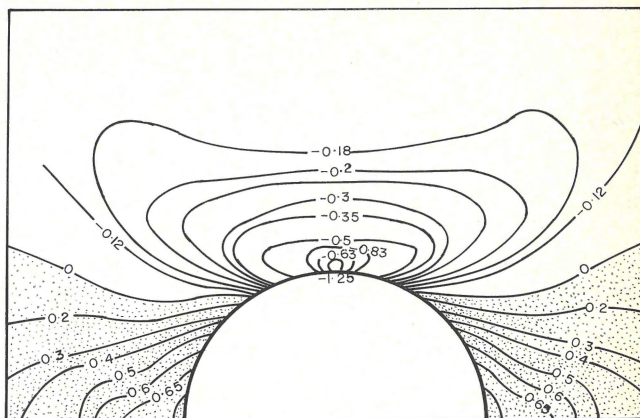


Fig. 3
Dimension of maximum principal stress around a rigid circular inclusion under uniaxial stress. The dotted regions are the areas of tensile stress. The numerical values are ratios of greatest principal stress to applied stress (P_1).

required values of the real constants are:
 $A = -2; B = 0; C = 1$ (13)

Finally an expression for the resolved stresses ($\sigma_r, \sigma_\theta, \tau_{r\theta}$) in the material around a rigid circular inclusion is obtained by substituting the values of real constants into eq. (12):

$$\begin{aligned} \sigma_r &= \frac{1}{2}P_1 + \frac{1}{2}P_1 \left(1 + \frac{4R^2}{r^2} - \frac{3R^4}{r^4}\right) \cos 2\theta \\ \sigma_\theta &= \frac{1}{2}P_1 - \frac{1}{2}P_1 \left(1 - \frac{3R^4}{r^4}\right) \cos 2\theta \\ \tau_{r\theta} &= -\frac{1}{2}P_1 \left(1 - \frac{2R^2}{r^2} + \frac{3R^4}{r^4}\right) \sin 2\theta \end{aligned} \quad \dots\dots\dots (14)$$

Hence from the above resolved stresses the distribution of the principal stresses (σ_1 and σ_3) and their orientation (Ω) can be easily evaluated from their standard relationship:

$$\begin{aligned} \sigma_1 &= \frac{\sigma_r + \sigma_\theta}{2} + \frac{1}{2} [(\sigma_r - \sigma_\theta)^2 + 4 \tau_{r\theta}^2]^{\frac{1}{2}} \\ \sigma_3 &= \frac{\sigma_r + \sigma_\theta}{2} - \frac{1}{2} [(\sigma_r - \sigma_\theta)^2 + 4 \tau_{r\theta}^2]^{\frac{1}{2}} \\ \Omega &= \frac{1}{2} \tan^{-1} \frac{2 \tau_{r\theta}}{\sigma_r - \sigma_\theta} \end{aligned} \quad \dots\dots\dots (15)$$

Stress trajectories and fracture pattern

Shear fractures developed at an angle Φ of the principal compression direction where $\Phi = \pm (45^\circ - \varphi_1/2)$. φ_1 is the angle of internal friction of the material (JAEGER & COOK, 1969). The results of many experiments show that, irrespective of the rock type, the value of φ_1 is always positive and less than 45° . HAFNER (1951) suggested that a satisfactory indication of the potential shear fracture pattern can be obtained by constructing lines at 30° to the compressive stress trajectories.

The direction of principal stresses around a rigid inclusion was calculated from equations (14) and (15) with the help of a computer and the stress trajectories were plotted in Fig. 2. The potential shear fractures which might develop in the matrix if it were to behave in a brittle manner are shown by broken lines in Fig. 2.

Distribution of the principal stresses and their influence in the formation of pressure shadows and pressure fringes

The values of maximum (σ_1) and minimum (σ_3) principal stress for an applied stress (P_1) are evaluated and the variation in σ_1 around a rigid circular inclusion is illustrated in Fig. 3. The variations are symmetrically distributed around the inclusion. High local compressive stresses are found on the side of the inclusion facing the greatest regional compression and high tensile stresses are found on the side facing normal to the greatest regional compression.

It is well known that tension fractures can be developed in the regions of tensile stress zone where $\sigma_1/P_1 > 0$ (dotted area in Fig. 3). Tension fractures developed in this area might be the deposition sites of material derived from the surrounding area by the process of pressure solution and mineral migration.

INTERPRETATION OF THE RESULTS AND THEIR GEOLOGICAL IMPLICATIONS

Using equations developed in the previous section the state of stress around a circular inclusion can be determined for any value of σ_1 and σ_3 . The stress trajectories, variation in mean stress and principal stress differences can be determined and the geological implications of the stress pattern considered.

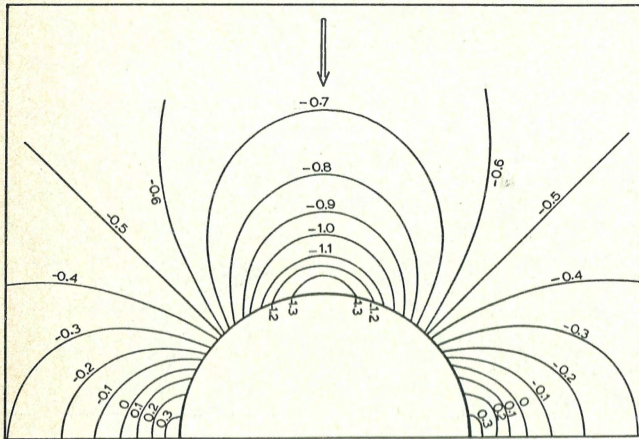


Fig. 4
Dimension of mean stress in the matrix around a rigid circular inclusion under uniaxial stress. The numerical values represent the ratios of mean stress [$\frac{1}{2}(\sigma_1 + \sigma_3)$] to applied stress (P_1). The magnitude varies proportionally with the applied compression.

'Pressure fringes' develop when the stresses are relatively high or the matrix is not very ductile. If the stresses are relatively low or the matrix is very ductile the inclusion/matrix contact does not open up and fractures do not form. In this situation minerals migrate into the low strain areas but are deposited in a more diffused manner within the matrix and form a 'pressure shadow'.

Role of mean stress in the development of pressure fringes and pressure shadows

Mean stress or pressure in the matrix around rigid circular inclusions has been evaluated from equation (15) and the variations are shown in figure 4. The highest value of mean stress lies along the plane parallel to the applied compressive stress and the lowest value of mean stress lies normal to it. The magnitude varies proportionally with the applied stress.

Field and experimental observations show that the pressure fringes and pressure shadows are formed in the regions which coincide with areas of low mean stress around the inclusion. Minerals migrate from high pressure zone into adjacent low pressure zone. It seems likely that new minerals would crystallise in the low mean stress zone to form pressure shadows and pressure fringes. The variation of mean stress governs the migration of material and the tensile zone near the object provides the area for deposition.

CONCLUSIONS

The basic equations of the stress theory have been extended to obtain solutions for the resolved stresses in the material around a rigid circular object loaded under plane strain. The stress trajectories obtained from the theoretical results have been used to evaluate the fracture patterns which are likely to develop if the matrix underwent brittle failure. High local tensile stress zones occur on the sides perpendicular to the greatest regional compression. These tensile zones are the regions in which pressure shadows and pressure fringes are likely to form.

The study of mean stress in the material around a circular rigid inclusion demonstrates that the highest value of mean stress lies along the plane parallel to the direction of greatest regional pressure and the lowest value lies perpendicular to it. The area of low mean stress and areas of tensile stress are found to coincide and are the regions suitable for the formation of pressure shadows and pressure fringes.

ACKNOWLEDGEMENTS

The author is indebted to Prof. J. G. Ramsay for his helpful supervision of the work which was undertaken at Imperial College, University of London as a part of Ph.D research. Thanks are due to Dr. J. W. Cosgrove for critically reading the manuscript. The receipt of Colomboplan scholarship during the time of the study is gratefully acknowledged.

REFERENCES

- Bain, G. W. 1933 Wall-rock mineralisation along Ontario gold deposits – *Econ. Geol.* 28: 705-743.
- Fairbairn, H. W. 1950 Pressure shadows and relative movement in shear zone – *Trans. Am. Geophys. Union* 31: 914-916.
- Frankel, J. J. 1957 Abraded pyrite crystals from the Witwatersrand gold mines – *Min. Mag.* 31: 392-401.
- Hafner, W. 1951 Stress distributions and faulting – *Bull. Geol. Soc. Am.* 62: 373-398.
- Jaeger, J. C. & N. G. W. Cook 1969 *Fundamentals of rock mechanics* – Chapman and Hall, 515 pp.
- Joplin, G. A. 1968 *A petrography of Australian metamorphic rock* – Angus and Robertson. (Sydney).
- Knopf, A. 1929 The mother lode system of California – *U.S. Geol. Surv. Prof. Paper* 157: 41-42.
- Miles, K. R. 1945 Metamorphic of the Jespar bars of W. Australia – *Quart. J. Geol. Soc. London* 52.
- Pabst, A. 1931 Pressure shadows and the measurement of the orientation of minerals in rocks – *Am. Mineral* 16: 55-70.
- Ramsay, J. G. 1967 *Folding and fracturing of rocks* – McGraw-Hill (New York), 568 pp.
- Spry, A. 1969 *Metamorphic textures* – Pergamon Press (Oxford), 350 pp.
- Strömgård, K. E. 1972 Stress distribution during formation of boudinage and pressure shadows. *Tectonophysics* 16: 215-248.